Phase front shapes in the KD_2PO_4 paraelectric-ferroelectric transition

1993 J. Phys.: Condens. Matter 5 2977

(http://iopscience.iop.org/0953-8984/5/18/020)

J. Phys.: Condens. Matter 5 (1993) 2977–2986. Printed in the UK

Phase front shapes in the KD_2PO_4 paraelectric–ferroelectric transition

Jean Bornarel† and Ryszard Cach‡

† Laboratoire de Spectrométrie Physique (Unité associée au CNRS 8), Université Joseph Fourier, BP 87, 38402 Saint-Martin-d'Hères Cédex, France

‡ Institute of Experimental Physics, University of Wrocław, ulica Cybulskiego 36, 50-205 Wrocław, Poland

Received 30 November 1992

Abstract. The competition between the elastic energy and the electrostatic energy induces particular shapes of the phase front at the KD_2PO_4 first-order transition. The coexistence of the two phases is reported for a paraelectric–ferroelectric transition; the relevant domain textures and dielectric properties are described. It is shown that the tilt angle between the phase front and the (001) plane never exceeds 22° in our experiments.

1. Introduction

Crystals of the KH_2PO_4 family show a transition between a tetragonal paraelectric phase (space group, $I\bar{4}2d$) at high temperatures, and an orthorhombic ferroelectric and ferroelastic phase (space group $mm2$) at low temperatures. In such compounds, the polarization P_z which is considered as the order parameter belongs to the same B_2 representation as the shear strain u_{xy}. Both u_{xy} and the birefringence Δn_{xy} for light propagating along the ferroelectric c axis are elements of a second-order tensor and also transform as B_2. Consequently P_z, u_{xy} and Δn_{xy} are proportional to each other, as verified experimentally (Bastie *et al* 1975, 1978). This property allows the use of an external shear stress σ_{xy} or an external electric field E_z to induce modifications in u_{xy} and P_z. Similarly, the ferroelectric domains in the low-temperature phase are also mechanical twins. The twin walls permissible by symmetry are the tetragonal planes (100) and (010) (Fousek and Janovec 1969). Many domain properties depend sensitively upon the mechanical energy (Bornarel 1987). For example, the long-range interaction between domains and between domain walls corresponds to interactions between the quasi-dislocations which systematically exist in domain walls not perfectly situated in the permissible walls. Many other characteristic properties of this crystal family are explained with the help of the mechanical energy and the electrostatic energy competition. The tetragonal–orthorhombic transition in the KDP crystal family is found to be second order for RbH_2PO_4, weakly first order for KH_2PO_4 and clearly first order for KD_2PO_4. Many experimental studies have been performed in order to understand the microscopic mechanism of the transition. DKDP crystals have been investigated using neutron diffraction (Nelmes *et al* 1985), x-ray measurements (Andrews and Cowley 1986), and polarization measurements (Sidnenko and Gladkii 1973), specific-heat data (Strukov *et al* 1968), and dielectric and electrocaloric properties (Reese 1969). On the other hand, there have been few studies at the microscopic level, i.e. observations of domain textures and phase coexistence. The purpose of the present paper is precisely to improve knowledge of the phase coexistence at the paraelectric–ferroelectric (PF) DKDP transition.

0953-8984/93/182977+10$07.50

The first information on phase coexistence was given by Zeyen *et al* (1976) who interpreted their neutron diffraction results with the help of PF lamellae whose phase fronts were planes perpendicular to the c ferroelectric axis. Optical observations confirm this hypothesis (Bastie *et al* 1980, Bachheimer *et al* 1981). More recently it has been shown that the coexistence of the ferroelectric and the paraelectric phases is an interesting example of the competition between the electrostatic energy and the elastic energy (Bornarel 1991, Bornarel and Cach 1991). The electrostatic energy would be minimized by a phase front parallel to the c ferroelectric axis which avoids the existence of charges on the front, whereas the elastic energy would be minimized by a phase front orientation perpendicular to the c axis because the u_{xx} and u_{yy}-values (10^{-4}) are lower than the u_{zz}-value (6.5×10^{-4}). The previous published results have confirmed this special competition state, showing typical phase front arrangements as zigzag fronts. The purpose of the present paper is to describe the coexistence phase in the cooling case, i.e. in a PF transition as well as in the heating case, i.e. in a ferroelectric–paraelectric (FP) transition. The ferroelectric domain texture is simultaneously observed and dielectric measurements are also performed.

2. Experimental procedures

The DKDP crystals were grown by slow cooling of a supersaturated solution of KDP and heavy water. The observed transition temperature of 210.8 ± 0.1 K corresponds to a deuteration concentration of 83% for the crystal. The weak tapering angle of the crystal (a few degrees), room-temperature optical studies and the dielectric properties lead to the conclusion that the samples were of good quality except for the nearby crystal seed. The sample was cut with a wire saw. The orientations of sample faces were verified with x-ray Bragg diffraction (accuracy of 1′) and each face was polished on a wet silk cloth with an alcohol and heavy-water solution. The sample dimensions were $a_1 = 2.5$ mm, $a_2 = 5$ mm and $c = 7$ mm. Semitransparent gold electrodes were evaporated on the c faces in the presence of Cr vapour to improve the adhesion onto the sample. The cryostat employed with a helium-gas exchange chamber allows optical observations along three perpendicular axes simultaneously with dielectric measurements. There is a small temperature gradient in the chamber and the temperatures of the sample a_1 faces differ by 0.2 K. However, at a given point the temperature can be regulated with an accuracy of a few 10^{-3} K. The cooling rate (and the heating rate too) in the last few kelvins around the transition was 10^{-2} K min^{-1}. The sample capacity and dissipation factor measured with an HP 4274 A impedance meter allow us to calculate ϵ_c' and ϵ_c'' values with relative accuracies of 3×10^{-3} and 10^{-2}, respectively (for an electric field 10^{-1} V cm^{-1} in amplitude and 4 kHz in frequency).

The observations in three perpendicular axes allow us to determine the arrangement of the two phases during their coexistence as illustrated in figure 1. The three directions of transmitted light across the sample are the tetragonal directions. Figure 1 shows typical arrangements of the front between the paraelectric and the ferroelectric phases and the corresponding images which are possible to observe by microscopy: the a_1 and a_2 images which allow us to reconstruct the phase front shape, and the c image in which the ferroelectric domains are observable and some limits of the phase fronts too. Because of the large thickness of the sample in the c direction, it is not easy to resolve the domain texture finely, but the direction of the domain walls appears clearly. The obvious data on the phase front obtained from the optical observations are the traces of the front on the sample boundaries. Moreover, it is also possible to obtain some contrasting images by particular orientations of the transmitted light as illustrated in figure 1 for the a_1 section.

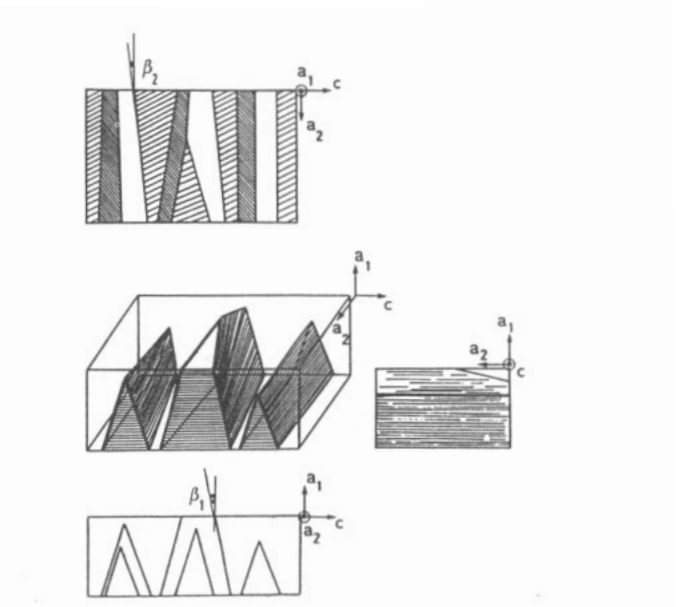

Figure 1. Schematic representation of a typical arrangement of phase fronts with domains in the ferroelectric phase. The images observed in the a_1 and a_2 directions allow us to reconstruct the phase front shape. In the representation the domains are drawn in perspective and in the c image. The shaded regions in the a_1 image illustrate the optical contrast.

This phenomenon is obviously used in the present study but the origin of this contrast is not discussed.

3. Results

3.1. The phase coexistence during a PF transition

A typical coexistence of phases is illustrated in figures 2 and 3 by a DKDP sample with a thermal gradient 0.08 K mm^{-1} along the a_1 direction. The photographs and the schematic illustrations in figure 2 allow us to describe the PF transition; at the beginning of the phase coexistence, ferroelectric nuclei appear at the sample ridge of the coolest a_1 sample face. These nuclei are dagger shaped and elongated in the a_2 direction, with a triangular section. These daggers often have the (001) plane as a bisector plane. The angle β_1 observed in an a_2 section between the phase front and the a_1 axis is about 10° or 15°. When the temperature is stabilized, i.e. controlled with a better accuracy than 10^{-2} K for $\frac{1}{2}$ h, no modification of the phase fronts arrangement is observable. If the sample is slowly cooled, the ferroelectric phase volume increases as follows. Firstly, the daggers fasten onto the coolest a_1 sample face and grow essentially in the c direction until they occupy all the a_1 sample face (during this lateral displacement of the dagger-shaped phase front, the β_1-values are conserved). Secondly, an increase in the volume of the ferroelectric region occurs in the a_1 direction, β_1 remaining constant. Then, the triangular sections of the daggers become trapezoidal when the daggers cross all the sample in the a_1 directions. If in the presence of a defect a dagger face attains a critical angle β_1^* (about 22°), another small dagger is created on this dagger face as shown in figure 2(*a*), 2, and the corresponding photograph in figure 2(*b*). Following

the creation of the small dagger, the two dagger faces make an angle β with the (001) plane of less than 15°. In such processes, the ferroelectric volume increases until the volume of the paraelectric phase in the sample becomes smaller than the volume of the ferroelectric phase. The dimensions of the paraelectric daggers decrease with decreasing temperature following an inverse process to that observed at the beginning of the PF transition. It is even possible to note that small daggers are sometimes created on a dagger face to avoid β_1-values higher than the critical β_1^*.

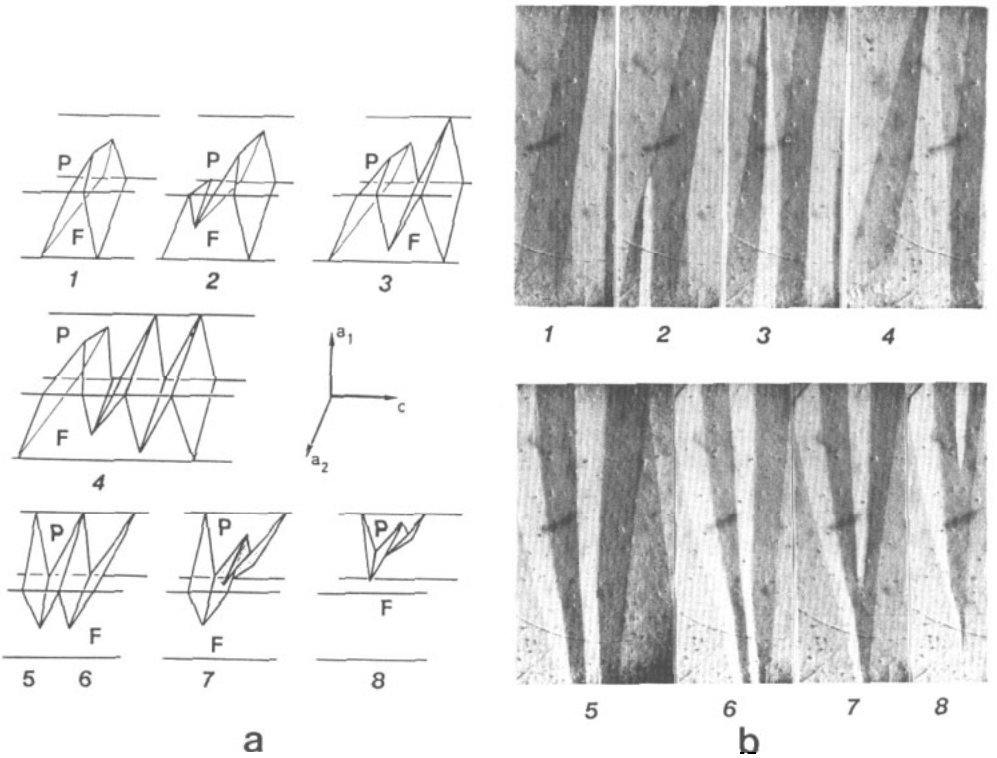

Figure 2. (*a*) Schematic representation of a PF transition with the dagger process; (*b*) corresponding photographs in the a_1 section.

It is interesting to note that the PF transition process happens usually with the creation of daggers with displacements of their faces in the c direction, maintaining the angle β_1 as previously described. However, situations such as that in figure 2(*b*), 4, can be observed. In such cases, the phase fronts which are the dagger faces also make an angle β_2 with the (001) plane, as an a_2 section. Similar to β_1, the β_2-values never exceed a critical value β_2^* (also equal to 22° in the present experimental conditions). What information on the ferroelectric domains during the PF transition does the observation along the c direction provide? At the beginning of the PF transition, with a ferroelectric volume equal, for example, to a tenth of the sample volume, no domains can be observed. It is difficult to conclude whether the ferroelectric phase has a monodomain nature or whether the domains cannot be observed by the optical methods used. The domains appear clearly when the ferroelectric phase volume reaches 20 or 30% of the sample volume. The domain walls are parallel to the dagger bases which are a_1 planes, as illustrated in figure 3(*b*). No important domain arrangements occur during the major part of the PF transition, but at the end of the PF transition, when the

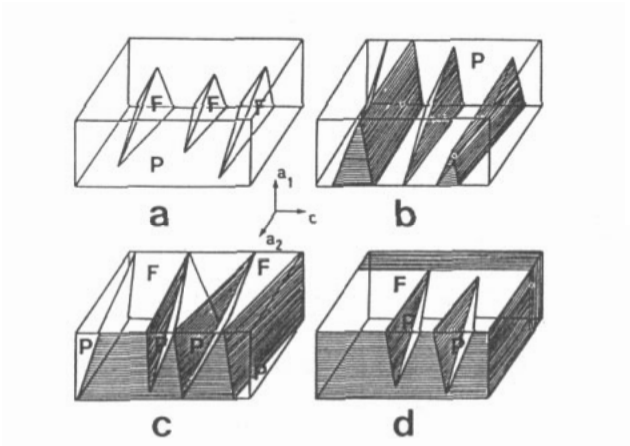

Figure 3. Schematic representation of a PF transition with the dagger process. The observed ferroelectric domains are drawn.

paraelectric daggers decrease so much that ferroelectric regions cross the whole sample in the a_1 and c directions (see figure 3(d)), rearrangements of the domain texture are observed. These texture modifications often allow different species of domains to exist, i.e. permissible walls in a_2 planes as well as in a_1 planes.

3.2. The phase coexistence during a FP transition

To obtain reproducible results for FP transitions, the temperature of the sample is kept a few kelvins below the transition for at least 10 h and then heated with a heating rate less than 10^{-2} K min^{-1}. In such experimental conditions, the FP transitions always occur with very regular modifications of the phase front in time and without observable domain texture arrangements, these textures only being scanned by the phase front. The modifications of the phase front shapes during the FP transition are similar to those previously described in the PF transition, and figures 4 and 5 illustrate the processes observed. In figure 4, daggers elongated in the a_2 direction, with their faces approximately parallel to this axis, change their volume by translation of their faces along the c direction. Different situations in the FP transition are illustrated in figure 4 by photographs simultaneously obtained along the a_1 axis and along the a_2 axis. It is possible to see that β_1 is always less than 15°, and β_2 is usually about zero.

Figure 5 illustrates another process which can be observed during a FP transition; a small number of daggers are created with β_1 always equal to about 15°. During the FP transition, β_2 increases until it reaches similar values. The disappearance of the ferroelectric phase happens either with small thin daggers as shown in figure 5 or by a phase front translation across the sample. In all cases the values of β_1 and β_2 do not exceed 20°.

3.3. Interaction between the phase front and the defects

No attention has yet been given to interactions between the phase front walls themselves. However, repulsive phenomena can be seen when a new dagger is created on a phase front wall such as in figure 2(b); the trace of the large dagger in the a_1 section increases in figure 2(b), 1, and becomes smaller in figure 2(b), 2, after the creation of the new dagger. However, if interactions between phase front walls exist, they do not appear as strongly as those between the ferroelectric domain walls for the same crystals.

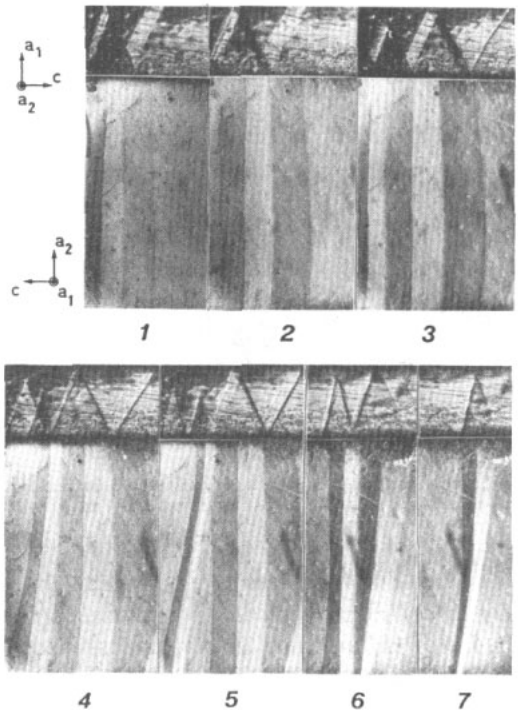

Figure 4. Different arrangements of the phase fronts during a FP transition. For each arrangement the upper photograph corresponds to the a_2 section and the lower photograph to the a_1 section.

In the same way, the interaction between the phase front and the sample boundaries is not clearly demonstrated. Except when the phase front is at a sample ridge, which could be a strained region, its motion seems similar near the sample boundary and in the bulk. However, the interaction is clear near the original pyramidal section of the seed where there is a large density of dislocations and mechanical defects. Figure 6 gives a typical example of the strange phase front shapes with ferroelectric regions completely surrounded by the paraelectric phase. The smooth shapes of this observed phase front and the non-detectable interactions between a phase front and the sample boundary lead us to suppose that the mechanical energy of the phase front itself seems relatively small.

3.4. Dielectric measurements

The dielectric constant ϵ_c' and the loss constant ϵ_c'' in the c-axis direction have been measured simultaneously with the optical observations, and their dependences on temperature are given in figure 7 for a PF transition, in a temperature range of a few kelvins around the transition. The variation in $\epsilon_c'(T)$ is well described in the paraelectric phase by a Curie–Weiss law $\epsilon_c' = C/T - T_0$ with $C = 3.5 \times 10^3$ K and $T_0 = 210.1 \pm 0.1$ K. In this high-temperature phase, the loss constant ϵ_c'' has a small value, lower than unity, as shown in figure 7(*b*). The increase in ϵ_c'' corresponds clearly to the appearance of the ferroelectric phase and thus can be used to detect when the phases coexist. On the contrary, during the first stage of the phase coexistence, ϵ_c' is still well described by the Curie–Weiss law as figure 7(*a*) shows. The variations in $\epsilon_c'(T)$ and $\epsilon_c''(T)$ during the phase coexistence are given in figure 8 for a PF transition and for a FP transition. The highest temperature of the phase coexistence region is reproducible with an accuracy of 10^{-2} K in successive PF or FP transitions (equal

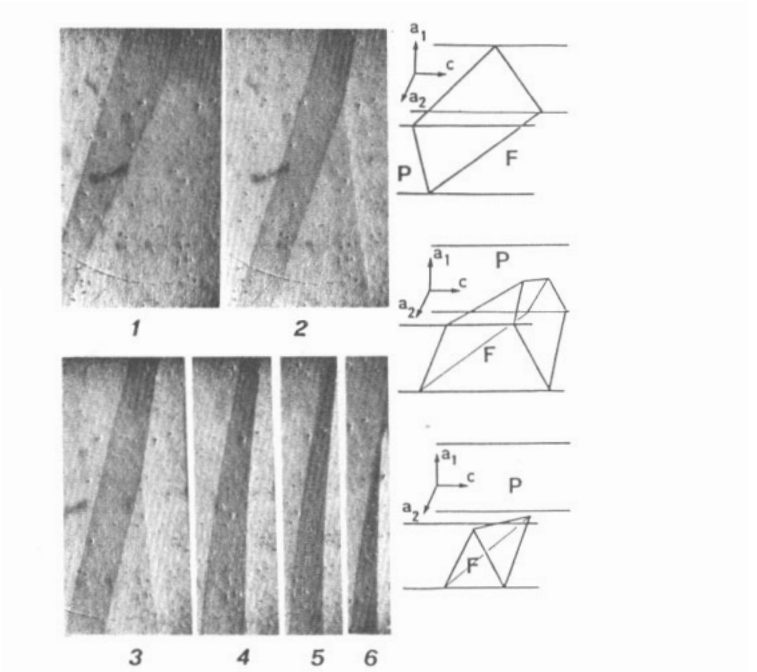

Figure 5. Photographs of a part of the sample observed along the a_1 direction during a FP transition. Three schematic representations help us to understand the phase front shape.

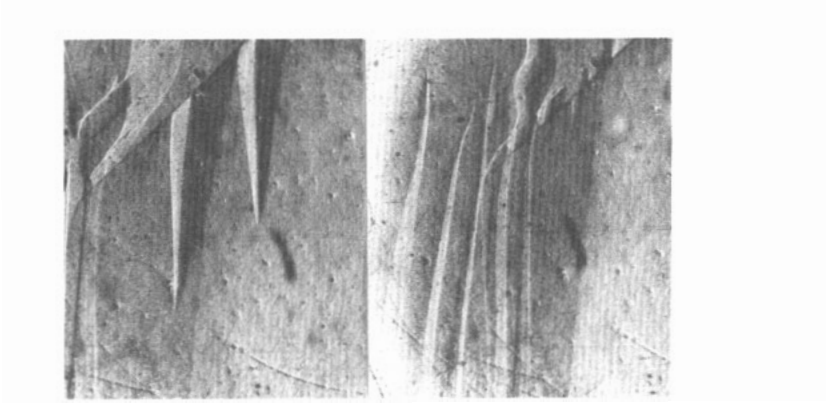

Figure 6. Strange phase front shapes in the bulk of the sample near the crystal seed. This photograph corresponds to the a_1 section.

to 210.90 ± 10^{-2} K). The lowest temperature, i.e. the limit between the coexistence region and the full ferroelectric state, can change to a few hundredths of a kelvin essentially for FP transitions where domain textures seem to play a role. The simultaneous optical observation of the phase front and of the domain texture allows us to comment on the $\epsilon_c'(T)$ and $\epsilon_c''(T)$ curves. Firstly, each modification in an $\epsilon_c''(T)$ curve is clearly correlated to a phase front displacement or modification. Secondly, the $\epsilon_c'(T)$ and $\epsilon_c''(T)$ values are larger in the PF transitions than in the FP transitions for a given temperature. As already explained (Bornarel 1987, 1991), during a PF transition, the domain texture exhibits many rearrangements of domain complexes (in a complex the domain walls are parallel to the same a tetragonal

direction) and modifications of the domain widths with decreasing temperature. This induces high dielectric and loss constant values. On the contrary, during a FP transition, the domain texture which has been stabilized at low temperatures does not change its configuration. The observation along the c axis shows only a reduction in the optical contrast with increasing temperature due to the enlargement of the domain wall widths.

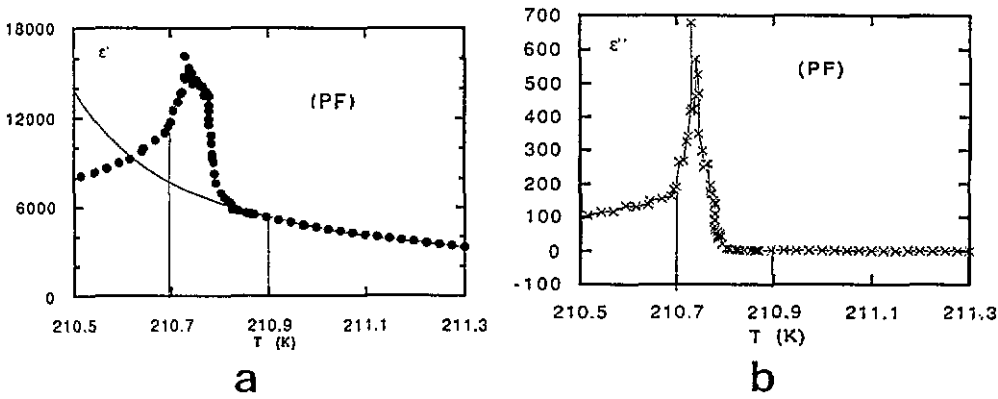

Figure 7. Variation in the dielectric properties with temperature around a PF transition: (*a*) dielectric constant ϵ_c' versus T; (*b*) loss constant ϵ_c'' versus T. The first appearance of the new phase (210.9 K) and completion of the phase transformation (below 210.7 K) are identified by thin straight vertical lines.

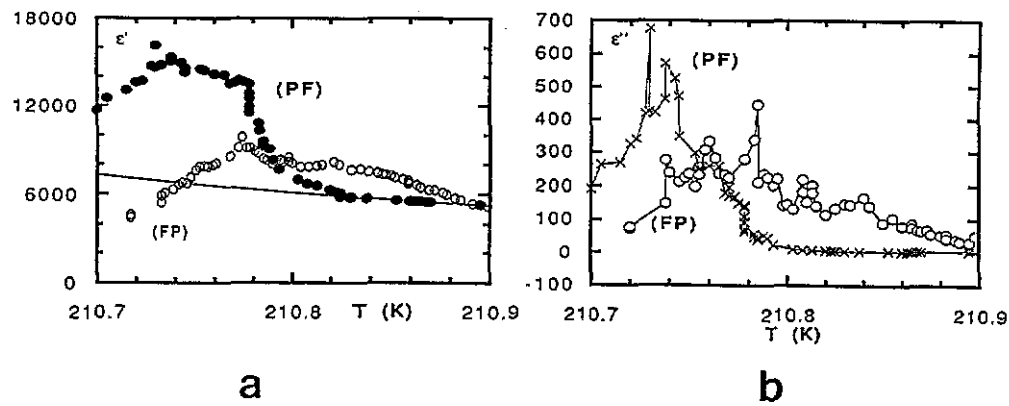

Figure 8. Variation in (*a*) ϵ_c' and (*b*) ϵ_c'' with T during a PF and a FP transition. The phases coexist in the temperature range 210.7–210.9 K. The Curie–Weiss law is satisfied in the PF transition above 210.83 K. The sharp drops in the curves correspond to abrupt displacements of the phase front.

4. Discussion

The coexistence of the ferroelectric phase and the paraelectric phase in DKDP has been observed in a temperature interval of 0.2 K. This temperature interval must change with the

experimental parameters such as the cooling (or heating) rate and the thermal gradient in the sample. The corresponding values in the present results are equal to 10^{-2} K min^{-1} and 0.08 K mm^{-1}, respectively in the a_1 direction. Further studies are necessary to improve knowledge of the coexistence temperature range, especially with a very small temperature rate and gradient.

The case reported confirms the greater importance of the elastic energy than of the electrostatic energy for the phase front orientation. Thus, if the phase front is not exactly in the (001) plane, which would correspond to the optimum situation for the elastic energy minimization in a simple model (Bastie *et al* 1980) using the Khatchaturyan (1967) analysis, it is very near; the angles β_1 and β_2 are usually equal to 10° or 15° and do not exceed 22°. It is necessary to study the phase coexistence in samples of different dimensions and with different thermal gradients in magnitude and orientation. It is possible, for example, to imagine that a thermal gradient parallel to the c axis induces a phase front in the (001) plane. Such experimental studies are in progress in our laboratory. It is also important to verify whether the critical angle β^* (= 22°) observed here corresponds to the experimental conditions used or whether it is the more general result of the energy minimization taking the phase front surface energy also into account. To progress in this direction, it is important to demonstrate whether the phase front contributes to the dielectric and loss constants, and then to separate these contributions from others.

The explanation of the following observation remains open: when the phase coexistence begins in a PF transition, in the major part of the ferroelectric region, ϵ_c' still follows a Curie–Weiss law (figure 7(a)) and it is only by accurate attention to ϵ_c'' values that the presence of the phase coexistence can be detected (figure 7(b)). The non-observability of the domain texture can be interpreted either as a monodomain ferroelectric region, or by such a thin domain texture that it was not possible to observe it optically. If the first hypothesis was confirmed, interesting models could be suggested using for example the role of the ferroelectric volume on the transition temperature because it has been known for a long time that the polydomain or the monodomain states are important for the existence of the transition (Jaccard *et al* 1953). Even better experimental results are necessary to discuss the different theories and models of interface orientations (Roytburd 1974, 1987, Sapriel 1975, Aleshko-Ozhevskij 1983, Chervonobrodov and Roytburd 1988). Finally, further experiments must clarify the possible correlation between the domain texture species, the orientations of the domain walls and the phase front shape.

References

Aleshko-Ozhevskij O P 1983 *Ferroelectrics* **48** 157

Andrews S R and Cowley R A 1986 *J. Phys. C: Solid State Phys.* **19** 615

Bachheimer J P, Bastie P, Bornarel J, Dolino G and Vallade M 1981 *Proc. Int. Conf. on Solid–Solid Phase Transformations* (Warrendale, PA: Metallurgical Society of AIME) pp 1533–7

Bastie P, Bornarel J, Dolino G and Vallade M 1980 *Ferroelectrics* **26** 789

Bastie P, Bornarel J, Lajzerowicz J, Vallade M and Schneider J R 1975 *Phys. Rev.* B **12** 5112

Bastie P, Lajzerowicz J and Schneider J R 1978 *J. Phys. C: Solid State Phys.* **11** 1203

Bornarel J 1987 *Ferroelectrics* **71** 255

—— 1991 *Phase Trans.* **34** 147

Bornarel J and Cach R 1991 *Ferroelectrics* **124** 345

Chervonobrodov S P and Roytburd A L 1988 *Ferroelectrics* **83** 109

Fousek J and Janovec V 1969 *J. Appl. Phys.* **40** 135

Jaccard C, Känzig W and Peter M 1953 *Helv. Phys. Acta* **26** 521

Khachaturyan A G 1967 *Sov. Phys.–Solid State* **8** 2131

Nelmes R J, Kuhs W F, Howard C J, Tibballs J E and Ryan T W 1985 *J. Phys. C: Solid State Phys.* **18** L1023, and papers of this team
Reese W 1969 *Phys. Rev.* **181** 2905
Roytburd A L 1974 *Sov. Phys.–Usp.* **17** 326
—— 1988 *JETP Lett.* **47** 171
Sapriel J 1975 *Phys. Rev.* B **12** 5128
Strukov B A, Amin M and Kopchik V A 1968 *Phys. Status Solidi* **27** 741
Sidnenko E V and Gladkii V V 1973 *Sov. Phys.–Crystallogr.* **17** 861
Zeyen C, Meister H and Kley W 1976 *Solid State Commun.* **18** 5